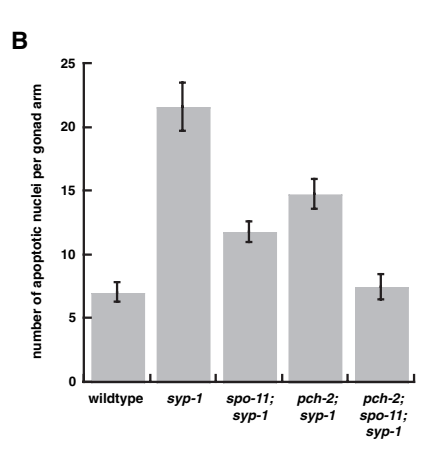


Fig. 4. The C. elegans gene pch-2 is required for the synapsis checkpoint but not the DNA damage/recombination checkpoint. (A) Mutation of pch-2 reduces apoptosis in meDf2/+ hermaphrodites but not in meDf2 or him-8 homozygotes. (B) Elimination of both pch-2 and spo-11 function restores apoptosis to wild-type levels in syp-1 mutants.



of checkpoints. In light of our evidence for conservation of pch-2 function from yeast to worms, defects in synapsis may also directly trigger meiotic arrest in budding yeast.

Unsynapsed sex chromosomes can activate a p53-independent meiotic checkpoint in mammals (2). Moreover, Spo11<sup>-/-</sup> mutant mice still exhibit spermatocyte death (3) and oocyte loss that is distinguishable from the apoptosis induced by mutations of DSB processing enzymes (4). Although direct experimental evidence is still lacking, it is likely that some loss of gametes in Spo11<sup>-/-</sup> mutant mice may result from their synaptic failures.

Our results demonstrate that synapsis can be monitored independently of recombination defects to ensure the accuracy of the meiotic divisions and prevent the production of aneuploid gametes. Further elucidation of this mechanism in C. elegans will likely shed light on the basis of human infertility, particularly in males, which has been linked to synaptic defects during meiotic prophase (29).

## References and Notes

- 1. G. S. Roeder, J. M. Bailis, Trends Genet. 16, 395 (2000).
- T. Odorisio, T. A. Rodriguez, E. P. Evans, A. R. Clarke, P. S. Burgoyne, Nat. Genet. 18, 257 (1998)
- 3. F. Baudat, K. Manova, J. P. Yuen, M. Jasin, S. Keeney, Mol. Cell 6, 989 (2000).
- 4. M. Di Giacomo et al., Proc. Natl. Acad. Sci. U.S.A. 102, 737 (2005)
- C. N. Giroux, M. E. Dresser, H. F. Tiano, Genome 31,
- 6. P. J. Romanienko, R. D. Camerini-Otero, Mol. Cell 6, 975 (2000).

- 7. A. F. Dernburg et al., Cell 94, 387 (1998).
- 8. A. J. MacQueen et al., Cell, in press. 9. A. M. Villeneuve, Genetics 136, 887 (1994).
- 10. T. L. Gumienny, E. Lambie, E. Hartwieg, H. R. Horvitz,
- M. O. Hengartner, Development 126, 1011 (1999). 11. J. Yuan, S. Shaham, S. Ledoux, H. M. Ellis, H. R. Horvitz, Cell 75, 641 (1993).

- 12. S. Shaham, H. R. Horvitz, Genes Dev. 10, 578 (1996). 13. M. C. Abraham, S. Shaham, Trends Cell Biol. 14, 184 (2004).
- 14. M. P. Colaiacovo et al., Dev. Cell 5, 463 (2003).
- 15. A. J. MacQueen, M. P. Colaiacovo, K. McDonald, A. M. Villeneuve, Genes Dev. 16, 2428 (2002).
- 16. E. R. Hofmann et al., Curr. Biol. 12, 1908 (2002).
- 17. S. J. Boulton et al., Curr. Biol. 14, 33 (2004).
- 18. W. B. Derry, A. P. Putzke, J. H. Rothman, Science 294, 591 (2001)
- 19. B. Schumacher, K. Hofmann, S. Boulton, A. Gartner, Curr. Biol. 11, 1722 (2001).
- 20. C. M. Phillips et al., Cell, in press.
- 21. F. Couteau, K. Nabeshima, A. Villeneuve, M. Zetka, Curr. Biol. 14, 585 (2004).
- 22. W. G. Kelly et al., Development 129, 479 (2002).
- 23. B. J. Meyer, Trends Genet. 16, 247 (2000).
- 24. K. C. Reddy, A. M. Villeneuve, Cell 118, 439 (2004).
- 25. A. Gartner, S. Milstein, S. Ahmed, J. Hodgkin, M. O. Hengartner, Mol. Cell 5, 435 (2000).
- 26. P. A. San-Segundo, G. S. Roeder, Cell 97, 313 (1999).
- 27. V. Reinke et al., Mol. Cell 6, 605 (2000).
- 28. R. S. Cha, B. M. Weiner, S. Keeney, J. Dekker, N. Kleckner, Genes Dev. 14, 493 (2000).
- 29. S. Egozcue et al., J. Assist. Reprod. Genet. 17, 307 (2000).
- 30. Materials and methods are available as supporting material on Science Online.
- 31. bcls39 (P<sub>lim</sub>::ced-1::GFP) and hus-1(op241) were provided by B. Conradt and M. Hengartner, respectively. The pch-2(tm1458) deletion was isolated by the Japanese National Bioresource for C. elegans. Many of the strains were provided by the Caenorhabditis Genetics Center. We thank S. Biggins, D. Smith, B. Brown, and members of the Dernburg lab for critical reading of the manuscript. This work was supported by an NIH/Ruth L. Kirschstein Individual National Research Service Award (1 F32 GM67408-01A1) to N.B. and NIH grant 1 R01 GM/CA655591-01 and Burroughs Wellcome Career Award 1000950 to A.F.D.

### **Supporting Online Material**

www.sciencemag.org/cgi/content/full/310/5754/1683/

Materials and Methods Figs. S1 to S3 References

15 July 2005; accepted 1 November 2005 10.1126/science.1117468

# **Snapshot of Activated G Proteins** at the Membrane: The $G\alpha_q$ -GRK2-G $\beta\gamma$ Complex

Valerie M. Tesmer, 1,2 Takeharu Kawano, 3\* Aruna Shankaranarayanan, 1,2\* Tohru Kozasa, 4 John J. G. Tesmer<sup>1,2</sup>†

G protein-coupled receptor kinase 2 (GRK2) plays a key role in the desensitization of G protein-coupled receptor signaling by phosphorylating activated heptahelical receptors and by sequestering heterotrimeric G proteins. We report the atomic structure of GRK2 in complex with  $G\alpha_a$  and  $G\beta\gamma$ , in which the activated G  $\alpha$  subunit of  $\textbf{G}_{\textbf{q}}$  is fully dissociated from  $\textbf{G}\beta\gamma$  and dramatically reoriented from its position in the inactive  $G\alpha\beta\gamma$  heterotrimer.  $G\alpha_a$  forms an effector-like interaction with the GRK2 regulator of G protein signaling (RGS) homology domain that is distinct from and does not overlap with that used to bind RGS proteins such as RGS4.

G protein-coupled receptors (GPCRs) are involved in a vast array of physiological processes, and the molecular basis for how signals are passed from activated receptors, through heterotrimeric G proteins ( $G\alpha\beta\gamma$ ), and then to downstream effectors has been the subject of intense investigation (1, 2). Crystal structures of inactive rhodopsin (3, 4) and the Ga $\beta\gamma$  heterotrimer (5, 6) have been determined, as have structures of activated Ga and GBy subunits

bound to various effector targets (7–10). These atomic models provide the first and last frames, respectively, of a molecular signaling movie that describes the course of heterotrimeric G protein signaling. The three switch regions of the Ga subunit play key roles, changing conformation depending on whether guanosine diphosphate (GDP) or guanosine triphosphate (GTP) is bound. In the G $\alpha$ B $\gamma$  heterotrimer, G $\alpha$ is bound to GDP, and switch II is sequestered by Gβγ (Fig. 1, A and B). On activation of Gα, GTP is bound; switch II dissociates from Gβy; and switches I, II, and III adopt a conformation appropriate for binding effectors and RGS proteins (7, 11, 12). The events that occur between the first and last frames of this molecular signaling movie are not well understood. Although receptor recognition of Gαβγ appears to be mediated primarily by the Cterminal region of the Ga subunit (13, 14), fundamental issues remain unresolved, including how activated GPCRs manipulate Gαβγ to mediate nucleotide exchange on  $G\alpha$  (15, 16); whether Gα, Gβγ, and GPCRs remain associated after activation (17-19); and how G protein subunits and their effector complexes are arranged at the membrane during signal transduction.

G protein-coupled receptor kinase 2 (GRK2) initiates phosphorylation-dependent desensitization of GPCRs (20, 21) by phosphorylating the C-terminal tail or third intracellular loop of activated GPCRs (22). GRK2 also can inhibit GPCR signaling via phosphorylationindependent mechanisms (23, 24), including sequestration of  $G\alpha_{q/11/14}$  subunits with its RGS homology (RH) domain (25–28) and G $\beta\gamma$  with its pleckstrin homology (PH) domain (29, 30). The crystallographic structure of GRK2 in complex with GBy suggested that the arrangement of its kinase, RH, and PH domains is compatible with the simultaneous recognition of activated receptor,  $G\alpha_q$ , and  $G\beta\gamma$ , respectively (9). The structure of a  $G\alpha_q$ -GRK2-G $\beta\gamma$  complex should therefore reveal the configuration of  $G\alpha$  and  $G\beta\gamma$  subunits as they engage a single protein target and provides another snapshot of the events that unfold after GPCR

 $G\alpha_q$  was overexpressed in insect cells as a soluble chimera (henceforth referred to as  $G\alpha_{i/q}$ ) in which the wild-type N-terminal helix was replaced with that of  $G\alpha_{i1}$  (31, 32).  $G\alpha_{i/q}$  bound GRK2 in an  $AlF_4^-$ -dependent manner (fig. S1), and the resulting  $G\alpha_{i/q}$ -GDP·Mg<sup>2+</sup>-

AlF<sub>4</sub> -GRK2 complex could be crystallized in the presence of a soluble mutant of  $G\beta_1\gamma_2$  (fig. S2). The resulting  $G\alpha_{i/q}$ -GRK2-G $\beta\gamma$  complex was solved by molecular replacement with the use of x-ray diffraction data extending to 3.1 and 4.5 Å spacings in the best and worst reciprocal lattice directions, respectively (table S1) (31).

In the  $G\alpha_{i/q}$ -GRK2-G $\beta\gamma$  complex, GRK2 serves as a scaffold for the activated heterotrimeric G proteins, with  $G\alpha_{i/q}$ -GDP·Mg<sup>2+</sup>·AlF<sub>4</sub> bound to the RH domain and G $\beta\gamma$  bound to the PH domain (Fig. 1, C and D). The switch regions of  $G\alpha_{i/q}$  adopt a conformation typical of other activated G $\alpha$  subunits (fig. S3), and  $G\alpha_{i/q}$ -bound GRK2-G $\beta\gamma$  differs only subtly from GRK2-G $\beta\gamma$  alone (see supporting online text). The G $\alpha$  subunit, however, undergoes a dramatic  $\sim$ 105° rotation from its position in the G $\alpha\beta\gamma$  heterotrimer to engage GRK2 (Figs. 1 and 2; movies S1 and S2).

In doing so, the regions of  $G\alpha$  believed to be adjacent to the membrane in  $G\alpha\beta\gamma$  (i.e., the N and C termini) are rotated away, such that switch I, switch II, linker 1, and the  $\alpha B-\alpha C$ loop are closest to the predicted membrane surface, although ~30 Å removed (Fig. 2). It is not clear whether this reorientation of  $G\alpha_{i/q}$ is GRK2-specific or if it could also represent the position of other activated, effectorbound  $G\alpha$  subunits at the membrane. We note that whereas structures of  $G\alpha$ , in complex with phosphodiesterase- $\gamma$  (PDE $\gamma$ ) and G $\alpha_{13}$  in complex with p115-Rho guanine nucleotide exchange factor (p115RhoGEF) are compatible with the predicted membrane surface when superimposed on GRK2-bound  $G\alpha_{i/a}$ , the  $G\alpha_s$ adenylyl cyclase complex is not (7,  $\dot{8}$ , 10). G $\beta\gamma$ also undergoes an apparent ~22° rotation from its position in the Gαβγ heterotrimer (compare Fig. 1, A and C), which was also evident in the GRK2-Gβγ structure (9).

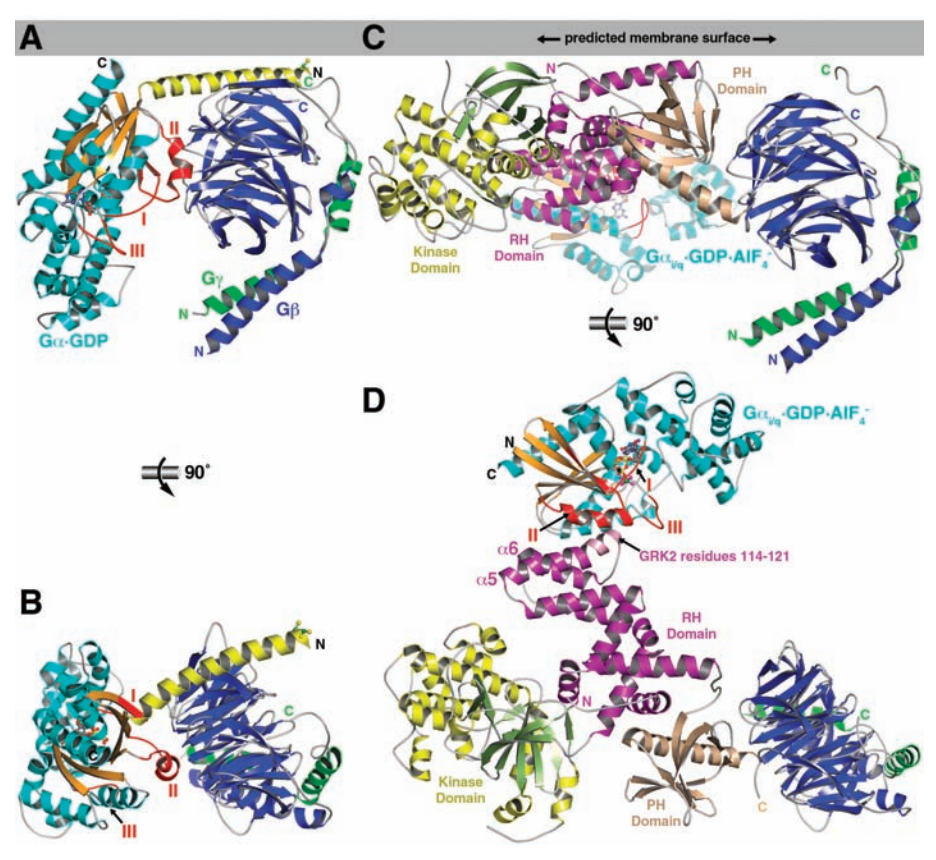


**Fig. 1.** Comparison of the inactive  $G\alpha\beta\gamma$  heterotrimer and the  $G\alpha_{i/q}$ –GRK2-Gβ $\gamma$  complex. (A) Side view of  $G\alpha_q\beta\gamma$ .  $G\alpha_g\beta\gamma$  was homology modeled by using the structure of  $G\alpha_i\beta_1\gamma_2$  (5). The expected membrane surface is modeled as a gray rectangle that extends out from the plane of the figure (31), and the heterotrimer is oriented as proposed in (6).  $G\alpha_q$  is cyan with orange β-strands, Gβ is blue, and G $\gamma$  is green. The three switch regions (labeled I, II, and III) and the N-terminal helix of  $G\alpha_q$  are red and yellow, respectively. GDP and  $G\alpha_q$ –Cys $^9$  and Cys $^{10}$ , which can be palmitoylated, are shown as ball-and-stick models. (B) Top view of  $G\alpha_q\beta\gamma$  from the perspective of the modeled membrane surface. (C) Side view of the  $G\alpha_{i/q}$ -GRK2-Gβ $\gamma$  complex. For purposes of comparison, GRK2-bound  $G\beta\gamma$  was centered in the same position as Gβ $\gamma$  in panel (A). The chimeric N-terminal helix of GRK2-bound  $G\alpha_{i/q}$  is disordered in the crystal structure. The kinase domain of GRK2 is yellow with olive β strands, the RH domain is purple, and the PH domain is tan. Mg $^{2+}$  (black sphere) and AIF $_4^{--}$  (green and magenta) are bound in the active site of  $G\alpha_{i/q}$ . (D) Top view of the  $G\alpha_{i/q}$ -GRK2-Gβ $\gamma$  complex from the same orientation as (B). Residues 114 to 121 in  $\alpha$ 5 of GRK2 (shaded pink) alter their conformation upon docking with the effector-binding pocket of  $G\alpha_{i/q}$  (see SOM text).

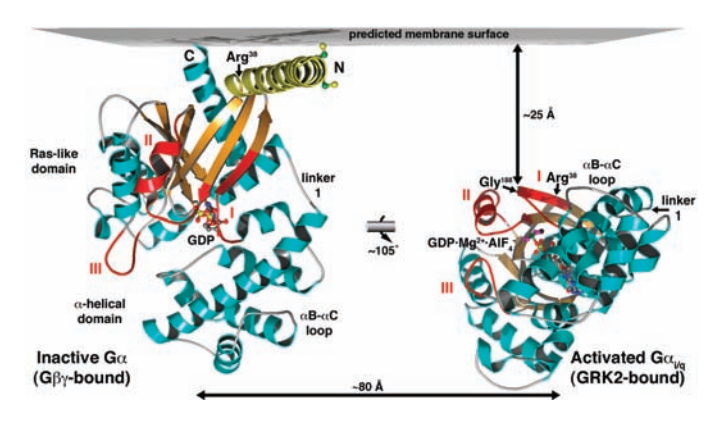
<sup>&</sup>lt;sup>1</sup>Institute for Cellular and Molecular Biology, Department of Chemistry and Biochemistry, University of Texas at Austin, Austin, TX 78712, USA. <sup>2</sup>Life Sciences Institute, Department of Pharmacology, University of Michigan, Ann Arbor, MI 48109, USA. <sup>3</sup>Department of Anatomy and Cell Biology and <sup>4</sup>Department of Pharmacology, University of Illinois, Chicago, IL 60612, USA.

<sup>\*</sup>These authors contributed equally to this work. †To whom correspondence should be addressed. E-mail: johntesmer@umich.edu

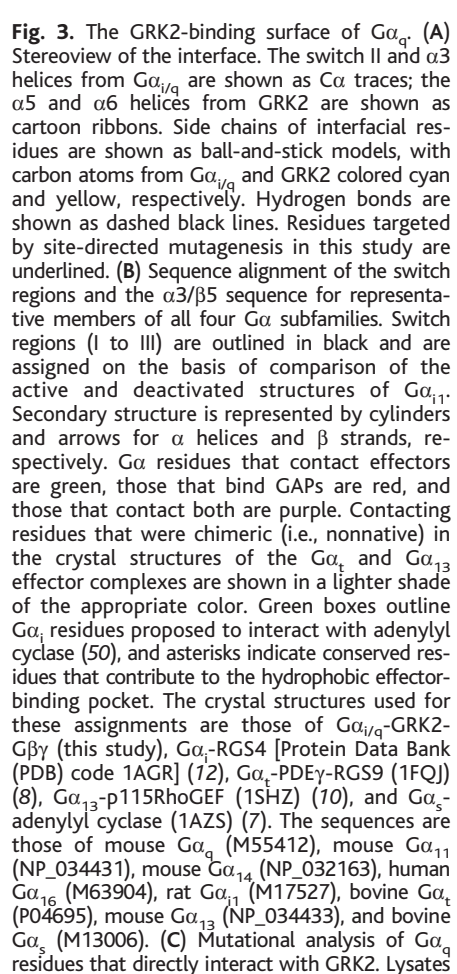
In Gαβγ, the N terminus of Gα forms a single, extended α helix that interacts with Gβ and, presumably, with the membrane via basic residues and/or lipid modifications (Fig. 1, A and B) (5, 6, 33). Interpreting the role of this helix in our structure is problematic because it is both chimeric and disordered. However, the first observed residue of  $G\alpha_{i/q}$ , corresponding to  $G\alpha_q$ -Arg<sup>38</sup>, is sufficiently removed from the predicted membrane surface (~30 Å) and from its position in the  $G\alpha\beta\gamma$  heterotrimer (~80 Å) to suggest that the N-terminal helix is at least partially dissociated from the membrane and completely dissociated from  $G\beta\gamma$  (Fig. 2).

The  $G\alpha_{i/q}$ -GRK2 interface buries  $\sim 1700~\text{Å}^2$  of accessible surface area and involves  $\alpha 2$  (switch II),  $\alpha 3$ , and the  $\alpha 3$ - $\beta 5$  loop of  $G\alpha_{i/q}$ , as well as the  $\alpha 5$  and  $\alpha 6$  helices of the GRK2 RH domain (Figs. 1D and 3A). Within the interface, hydrogen bonds are formed between the hydroxyl of  $G\alpha_q$ -Tyr<sup>261</sup> and the side chains of GRK2-Asp<sup>110</sup> and -Arg<sup>106</sup>, as well

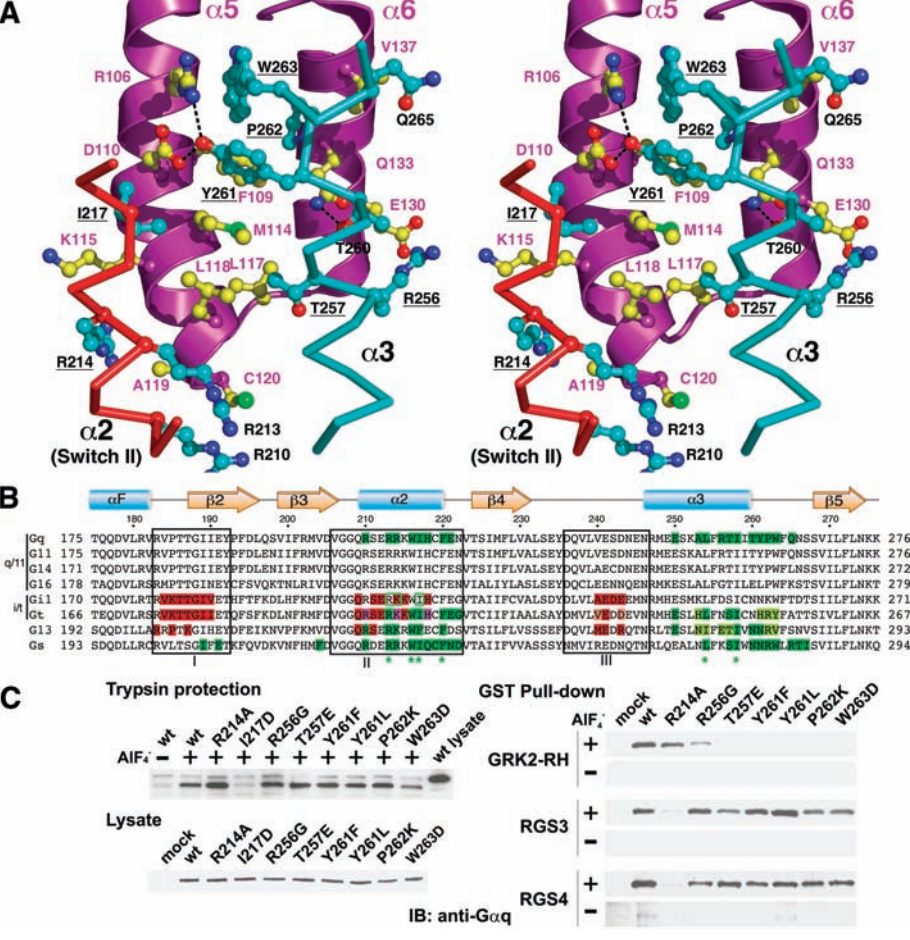
Fig. 2. Changes in the orientation of  $G\alpha_a$  on activation and binding of GRK2. The model of Gβγ-bound Gα GDP and the structure of GRK2-bound  $G\alpha_{i/q}$ -GDP-  $Mg^{2+}$ -AlF $_4^-$  are viewed from a direction roughly 90° around a vertical axis from those of Fig. 1, A and C, respectively. The  $G\alpha$  subunits were positioned by translationally centering the  $G\beta\gamma$  subunits of their respective complexes



along the plane of the modeled membrane (Fig. 1). On binding GRK2,  $G\alpha_{i/q}$  rotates by  $\sim 105^\circ$  such that Gly<sup>188</sup> in switch I of GRK2-bound  $G\alpha_{i/q}$  becomes the closest residue to the modeled membrane surface ( $\sim 25$  Å below). The most N-terminal residue observed in GRK2-bound  $G\alpha_{i/q}$ , Arg<sup>38</sup>, which is expected to be adjacent to the membrane in  $G\alpha\beta\gamma$ , is displaced by  $\sim 30$  Å from the membrane. However, the native N-terminal helix of  $G\alpha_q$  is sufficiently long (37 residues,  $\sim 55$  Å long) to allow the palmitoylation sites at Cys<sup>9</sup> and Cys<sup>10</sup> to be adjacent to the membrane. If one assumes that  $G\alpha$  and  $G\beta\gamma$  derive from a single heterotrimer,  $G\alpha_q$ -Arg<sup>38</sup> also translates  $\sim 80$  Å away from its position in the  $G\alpha\beta\gamma$  heterotrimer (Fig. 2), and the fully extended wild-type N-terminal helix of  $G\alpha_q$  would fall short of contacting  $G\beta\gamma$ . Therefore, activated  $G\alpha_q$  dissociates partially, if not completely, from the membrane and entirely from  $G\beta\gamma$ , at least when in complex with GRK2.



of HEK293 cells expressing  $G\alpha_q$  mutants were subjected to limited trypsin digestion in the presence and absence (shown only for wild type) of AlF $_q$  and immunoblotted with  $G\alpha_q$ -specific antibody (upper left) (31). The I217D mutation could not be protected from trypsin digestion and was judged nonfunctional. All  $G\alpha_q$  mutants expressed at a similar level com-



pared with wild-type  $G\alpha_q$  (lower left). Pull-down assays were performed by incubating lysates with 40 nM glutathione S-transferase (GST) fusion protein of either GRK2-RH, RGS3 (amino acids 313 to 519), or RGS4 either in the presence or absence of  $AlF_4^-$  and then detecting bound  $G\alpha_q$  with  $G\alpha_a$ -specific antibody (right).

as between the side chains of  $G\alpha_q$ -Thr<sup>260</sup> and GRK2-Gln<sup>133</sup>. The primary nonpolar interactions are made by the side chains of GRK2-Met<sup>114</sup>, Leu<sup>117</sup>, Leu<sup>118</sup>, and Cys<sup>120</sup>, which dock into a cleft formed between the  $\alpha 2$  (switch II) and  $\alpha 3$  helices of  $G\alpha_{i/q}$ . The residues of GRK2 that form the interface with  $G\alpha_{i/q}$  are essentially the same as those identified in previous studies, wherein mutation of Asp<sup>110</sup>, Arg<sup>106</sup>, and Leu<sup>118</sup> of the GRK2 RH domain eliminated  $G\alpha_q$  binding (34, 35).

Furthermore, the D110A mutation in GRK2 abrogates its ability to mediate phosphorylation-independent desensitization in vivo (36, 37). The GRK2-binding residues of  $G\alpha_{i/q}$  are analogous to those in  $G\alpha_s$  and  $G\alpha_t$  that bind adenylyl cyclase and PDE $\gamma$ , respectively (7, 8), and are among those previously implicated in the binding of phospholipase C- $\beta$  (PLC- $\beta$ ) (38, 39). Thus, the GRK2 RH domain binds  $G\alpha_{i/q}$  more like an effector than an RGS protein (8, 12) (Fig. 3B), a result that is con-

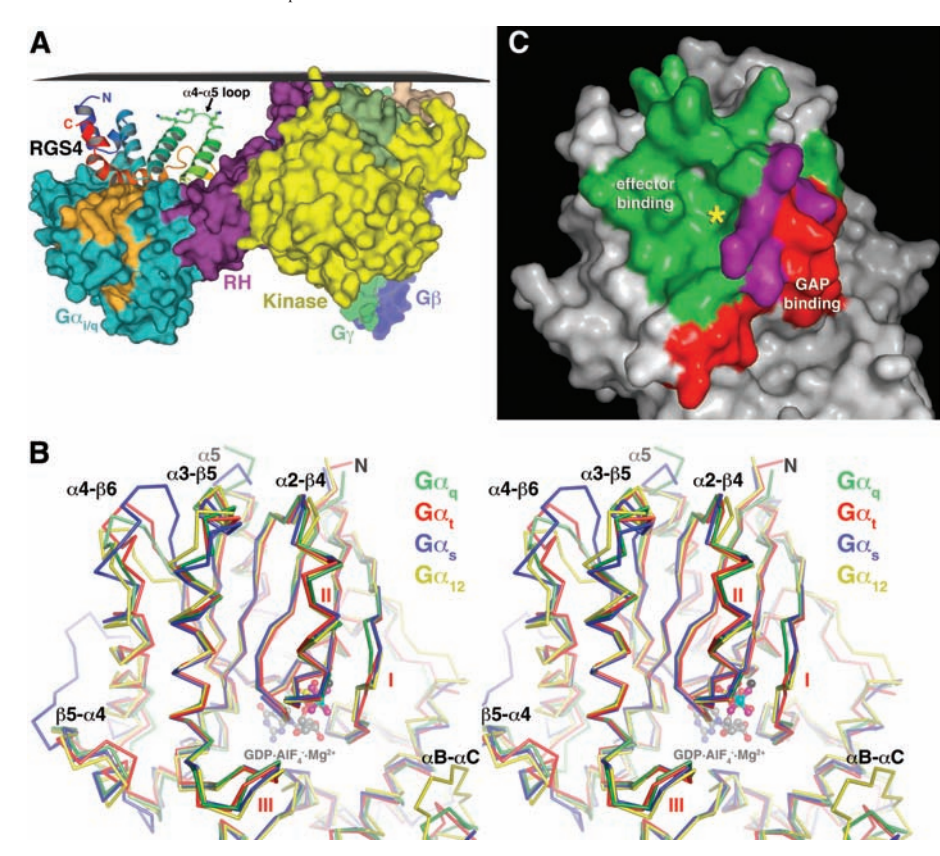


Fig. 4. Comparison of effector and GAP-binding sites among the four  $G\alpha$  subfamilies. (A) Model of RGS4 bound to the  $G\alpha_{1/a}$ -GRK2-G $\beta\gamma$  complex. RGS4 was positioned by superimposing  $G\alpha$ , of the  $G\alpha$ -RGS4 complex (12) with  $G\alpha_{i/a}$ . The docked RGS4 has no obvious steric overlaps with GRK2. The  $\alpha$ 4- $\alpha$ 5 loop and the N-terminal region of RGS4, which are both believed to interact with the cell membrane (51, 52), are juxtaposed with the membrane surface modeled for the  $G\alpha_{i/q}$ -GRK2-G $\beta\gamma$ complex. The  $G\alpha_{i/q}$ -GRK2-G $\beta\gamma$  complex is shown as a molecular surface with the same colors as in Fig. 1, except that the switch regions of  $G\alpha_{i/q}$  are not highlighted. RGS4 is colored in a spectrum from blue to red from its observed N and C termini (residues 51 and 178, respectively). The side chains of basic residues in its  $\alpha 4-\alpha 5$  loop believed to interact with phosphatidylinositol 3,4,5-trisphosphate (PIP<sub>3</sub>) (51), are shown as ball-and-stick models. (B) Structural alignment of Ras-like domains of activated  $G\alpha$  subunits. The region of  $G\alpha$  that encompasses the three switch regions was used for the alignment:  $G\alpha_a$  (this study, green), residues 183 to 261;  $G\alpha_{\star}$  (PDB code 1TAD, red), residues 174 to 252 (53);  $G\alpha_s^2$  (1AZS, blue), residues 201 to 279 (7); and  $G\alpha_{12}$  (1ZCA, yellow), residues 203 to 281 (32). The structure of activated  $G\alpha_{12}$  is used to represent the  $G\alpha_{12/13}$  family, because the  $G\alpha_{13}$  protein used in the p115RhoGEF complex is a  $G\alpha_{11}$  chimera within the effector-binding region (10). Overall,  $G\alpha_a$  is most similar to  $G\alpha_i$  and  $G\alpha_t$  (root mean square deviation of 1.0 Å for 303 analogous  $C^{\alpha}$  positions). The most structurally heterogeneous regions of  $G\alpha_q$  are the  $\beta$ 5- $\alpha$ 4 and  $\alpha$ 4- $\beta$ 6 loops in the Ras-like domain and, in the  $\alpha$ -helical domain, the  $\alpha$ B- $\alpha$ C loop. The distinct structures of the  $\alpha$ 4- $\beta$ 6 and  $\alpha$ B- $\alpha$ C loops may allow for specific recognition of G $\alpha$  subunits by receptors or guaninenucleotide exchange inhibitors, respectively (2, 54). In contrast, the tertiary structures of the switch regions, which dictate effector and GAP protein interactions, are well conserved. (C) Footprints of effector and GAP-binding sites on the molecular surface of  $G\alpha_{i/q}$ . Colors are assigned as in Fig. 3B. The yellow asterisk indicates the position of the hydrophobic pocket used by all characterized  $G\alpha$ effectors. As originally proposed on inspection of the  $G\alpha_s$ -adenylyl cyclase complex (7, 55), effectors and GAPs have apparently evolved to bind to distinct and generally nonoverlapping regions of the  $G\alpha$ subunit. Although the residues colored purple imply steric overlap, different surfaces of these residues are used to bind effectors and GAPs.

sistent with the facts that GRK2 efficiently binds  $G\alpha_q$ -GTP $\gamma$ S and does not exhibit significant guanosine triphosphatase (GTPase)—activating protein (GAP) activity toward  $G\alpha_q$  (25). Residues in switches I and III of  $G\alpha_q$  previously implicated in binding GRK2 (35) appear to play only an indirect role, perhaps by altering the structure or dynamics of switch II.

The R214A, I217D, T257E, Y261F, and W263D mutants of  $G\alpha_q$  (40) were generated to test the importance of these positions for binding GRK2 (Fig. 3C). The  $G\alpha_{\sigma}$ -T257E,  $G\alpha_{a}$ -Y261F, and  $G\alpha_{a}$ -W263D mutants completely abrogated binding, whereas the Gα<sub>a</sub>-R214A mutant retained its interaction with the GRK2 RH domain, and the I217D mutant was nonfunctional (Fig. 3C). The complete loss of binding caused by the subtle Y261F mutation emphasizes the importance of the hydrogen bonds formed by the hydroxyl of  $G\alpha_{\sigma}$ -Tyr<sup>261</sup>. Previously, it was shown that the  $G\alpha_a^3$ -I259A/ T260A/Y261A mutant stimulates PLC-β similarly to wild type and that the  $G\alpha_{q}$ -R256A/ T257A mutant is deficient (39). Therefore, whereas GRK2 and PLC-\$\beta\$ bind overlapping regions on  $G\alpha_{_{\textrm{\tiny q}}}$  , the residues of  $G\alpha_{_{\textrm{\tiny q}}}$  most critical for binding differ.

Next, the  $G\alpha_{q}$ -P262K, R256G, and Y261L mutants were created to test the role of these positions in dictating specificity of  $G\alpha_a$  for GRK2 (Fig. 3B). In other Gα subfamilies, the residue equivalent to  $G\alpha_q$ -Pro<sup>262</sup>, which packs between  $G\alpha_q$ -Trp<sup>263</sup>, GRK2-Leu<sup>136</sup>, and GRK2-Val<sup>137</sup> (Fig. 3A), is replaced by either arginine or lysine. As expected, the Ga<sub>a</sub>-P262K mutation abolished GRK2 binding (Fig. 3C). The  $G\alpha_{\text{q}}\text{-R256G}$  and  $G\alpha_{\text{q}}\text{-Y261L}$  mutants represent conversions of these residues to their equivalents in  $Ga_{16}$  (Fig. 3B), which does not bind GRK2 (28). The R256G mutation significantly reduced binding, whereas the Ga<sub>a</sub>-Y261L substitution eliminated binding (Fig. 3C). Therefore, residues 261 to 263 of  $G\alpha_{q}$ , and their equivalents in  $G\alpha_{11}$  and  $G\alpha_{14}$ , appear sufficient to dictate the Ga specificity

The Gα<sub>q</sub>-R214A mutation in switch II completely abolished binding to RGS3 and RGS4, but not to GRK2, emphasizing the importance of Gα<sub>a</sub>-Arg<sup>214</sup> in Gα-RGS protein recognition (8, 12). Strikingly, none of the mutations in  $G\alpha_{a}$ that affected GRK2 binding interfered with the binding of RGS proteins (Fig. 3C). Therefore,  $G\alpha_{\alpha}$  binds the GRK2 RH domain using a surface distinct from that used for binding RGS proteins. Indeed, when RGS4 is modeled in complex with  $G\alpha_{i/q}$ , there is no obvious steric overlap between RGS4 and GRK2 (Fig. 4A), which implies that  $G\alpha_{a}$  could bind two different RH domains at the same time: one as an effector (GRK2) and the other as a GAP (RGS protein). This model also predicts that the  $\alpha$ -helical domain of  $G\alpha_{\alpha}$  will form substantial contacts with RGS4 (and presumably RGS2) that are not possible in  $G\alpha_i$  or  $G\alpha_t$  owing to substitutions in aA and differences in the structure of the αB-αC loop (Fig. 4B). This novel interaction may help dictate the relative specificity of RGS4 and RGS2 for  $G\alpha_a$  (41).

Together with the Gα<sub>s</sub>-adenylyl cyclase,  $G\alpha_t$ -PDE $\gamma$ -RGS9, and  $G\alpha_{13}$ -p115RhoGEF complexes (7, 8, 10), the  $G\alpha_{i/q}$ -GRK2-G $\beta\gamma$  structure completes a survey of effector complexes representing the four Ga protein subfamilies (Fig. 4B). Comparison of these structures demonstrates that structurally diverse effectors recognize a highly localized region on each Ga subunit in a manner that does not necessarily exclude the binding of GAP domains (Figs. 3B and 4C). In each case, solventexposed hydrophobic side chains from the effector dock into a nearly invariant pocket formed between the N termini of the switch II (α2) and α3 helices of Gα (Fig. 3B; Fig. 4, B and C). Additional specificity-determining contacts are made with residues at the C-terminal ends of these helices and within the  $\alpha$ 2- $\beta$ 4 and α3-β5 loops (Fig. 3B). With the exception of the  $\alpha 3$ - $\beta 5$  loop in  $G\alpha_s$ , the tertiary structures of the effector interacting regions are well conserved (Fig. 4B), which implies that effector specificity in most Ga subunits is dictated by primary sequence and, at least in some cases, differences in electrostatic potential (fig. S4).

The physiological consequence and/or necessity of GRK2 binding both  $G\alpha_{\alpha}$  and  $G\beta\gamma$ is not known, but the nanomolar affinity of these interactions (25, 42, 43) and the expected close proximity of these proteins to each other while associated with the membrane suggest that a  $G\alpha_q$ -GRK2-G $\beta\gamma$  complex can form soon after a Gq-coupled receptor is activated. Simultaneous engagement of Ga and Gβγ is a characteristic shared among GRK2 and classic effectors like adenylyl cyclase and PLC-B. This, along with the observed effector-like interaction between GRK2 and  $G\alpha_a$  and the fact that heptahelical receptors directly stimulate the kinase activity of GRK2 (22), invokes the question of whether GRK2 can instigate its own signaling cascade. Potential downstream targets include insulin receptor substrate-1 (IRS-1) (44) and the cytoskeletal regulator ezrin (45), which can be phosphorylated by GRK2 in response to activation of G<sub>a</sub>-coupled receptors.

An increasing body of evidence suggests that GPCR signaling systems can function as preassembled complexes, which should allow

for efficient transmission and desensitization of extracellular signals (19). The  $G\alpha_{i/a}$ -GRK2-Gβγ structure strongly supports this hypothesis, at least in the case of G<sub>q</sub>-coupled receptors, with GRK2 harboring at least one additional protein-binding site for an activated receptor. The potential coassembly of this complex with RGS proteins like RGS4 and RGS2 (Fig. 4A) is intriguing in light of their reported association with receptor complexes (46–49). Defining the molecular basis for the interactions among GPCRs, RGS proteins, heterotrimeric G proteins, and GRK2 will be the focus of future

#### References and Notes

- 1. H. R. Bourne, Curr. Opin. Cell Biol. 9, 134 (1997).
- 2. T. M. Cabrera-Vera et al., Endocr. Rev. 24, 765 (2003).
- 3. K. Palczewski et al., Science 289, 739 (2000).
- 4. J. Li, P. C. Edwards, M. Burghammer, C. Villa, G. F. Schertler, J. Mol. Biol. 343, 1409 (2004).
- 5. M. A. Wall et al., Cell 83, 1047 (1995).
- 6. D. G. Lambright et al., Nature 379, 311 (1996).
- 7. J. Tesmer, R. Sunahara, A. Gilman, S. Sprang, Science **278**, 1907 (1997).
- 8. K. C. Slep et al., Nature 409, 1071 (2001).
- 9. D. T. Lodowski, J. A. Pitcher, W. D. Capel, R. J. Lefkowitz, J. J. Tesmer, Science 300, 1256 (2003).
- 10. Z. Chen, W. D. Singer, P. C. Sternweis, S. R. Sprang, Nat. Struct. Mol. Biol. 12, 191 (2005).
- 11. S. R. Sprang, Annu. Rev. Biochem. 66, 639 (1997).
- 12. J. J. G. Tesmer, D. M. Berman, A. G. Gilman, S. R. Sprang, Cell 89, 251 (1997).
- 13. B. R. Conklin, H. R. Bourne, Cell 73, 631 (1993).
- 14. A. Gilchrist, A. Li, H. E. Hamm, Sci. STKE 2002, pl1 (2002).
- 15. T. Iiri, Z. Farfel, H. R. Bourne, Nature 394, 35 (1998).
- 16. J. Cherfils, M. Chabre, Trends Biochem. Sci. 28, 13 (2003).
- 17. I. Azpiazu, N. Gautam, J. Biol. Chem. 279, 27709 (2004). 18. M. Frank, L. Thumer, M. J. Lohse, M. Bunemann, J. Biol.
- Chem. 280, 24584 (2005).
- 19. R. V. Rebois, T. E. Hebert, Receptors Channels 9, 169 (2003).
- 20. N. J. Freedman, R. J. Lefkowitz, Recent Prog. Horm. Res. 51, 319 (1996). 21. J. G. Krupnick, J. L. Benovic, Annu. Rev. Pharmacol.
- Toxicol. 38, 289 (1998). 22. J. A. Pitcher, N. J. Freedman, R. J. Lefkowitz, Annu.
- Rev. Biochem. 67, 653 (1998). 23. C. S. Pao, J. L. Benovic, Sci. STKE 2002, pe42 (2002).
- 24. J. M. Willets, R. A. Challiss, S. R. Nahorski, Trends Pharmacol. Sci. 24, 626 (2003).
- 25. C. V. Carman et al., J. Biol. Chem. 274, 34483 (1999).
- 26. M. Sallese, S. Mariggio, E. D'Urbano, L. Iacovelli, A. De Blasi, Mol. Pharmacol. 57, 826 (2000).
- 27. H. Usui et al., Int. J. Mol. Med. 5, 335 (2000).
- 28. P. W. Day, C. V. Carman, R. Sterne-Marr, J. L. Benovic, P. B. Wedegaertner, Biochemistry 42, 9176 (2003).
- 29. W. J. Koch, J. Inglese, W. C. Stone, R. J. Lefkowitz, J. Biol. Chem. 268, 8256 (1993).
- 30. W. J. Koch, B. E. Hawes, J. Inglese, L. M. Luttrell, R. J. Lefkowitz, J. Biol. Chem. 269, 6193 (1994).
- 31. Materials and methods are available as supporting material on Science Online.
- 32. B. Kreutz et al., Biochemistry, in press.
- E. J. Neer, L. Pulsifer, L. G. Wolf, J. Biol. Chem. 263, 8996 (1988).
- 34. R. Sterne-Marr et al., J. Biol. Chem. 278, 6050 (2003).

- 35. P. W. Day et al., J. Biol. Chem. 279, 53643 (2004).
- 36. J. M. Willets, S. R. Nahorski, R. A. Challiss, J. Biol. Chem. 280, 18950 (2005).
- 37. K. Iwata, J. Luo, R. B. Penn, J. L. Benovic, J. Biol. Chem. 280, 2197 (2005).
- 38. S. Arkinstall, C. Chabert, K. Maundrell, M. Peitsch, FEBS Lett. 364, 45 (1995).
- 39. G. Venkatakrishnan, J. H. Exton, J. Biol. Chem. 271, 5066 (1996).
- 40. Single-letter abbreviations for the amino acid residues are as follows: A, Ala; D, Asp; E, Glu; F, Phe; G, Gly; I, Ile; R, Arg; T, Thr; W, Trp; and Y, Tyr.
- 41. S. P. Heximer, N. Watson, M. E. Linder, K. J. Blumer, J. R. Hepler, Proc. Natl. Acad. Sci. U.S.A. 94, 14389 (1997). 42. J. A. Pitcher et al., Science 257, 1264 (1992)
- 43. K. Haga, T. Haga, J. Biol. Chem. 267, 2222 (1992).
- 44. I. Usui et al., Mol. Endocrinol. 19, 2760 (2005).
- 45. S. H. Cant, J. A. Pitcher, Mol. Biol. Cell 16, 3088 (2005).
- 46. W. Zeng et al., J. Biol. Chem. 273, 34687 (1998).
- 47. X. Xu et al., J. Biol. Chem. 274, 3549 (1999).
- 48. L. S. Bernstein et al., J. Biol. Chem. 279, 21248 (2004).
- 49. C. Hague et al., J. Biol. Chem. 280, 27289 (2005).
- 50. G. Grishina, C. H. Berlot, J. Biol. Chem. 272, 20619
- (1997). 51. S. G. Popov, U. M. Krishna, J. R. Falck, T. M. Wilkie,
- J. Biol. Chem. 275, 18962 (2000).
- 52. Y. Tu, S. Popov, C. Slaughter, E. M. Ross, J. Biol. Chem. 274, 38260 (1999).
- 53. J. Sondek, D. G. Lambright, J. P. Noel, H. E. Hamm, P. B. Sigler, Nature 372, 276 (1994).
- 54. R. J. Kimple, M. E. Kimple, L. Betts, J. Sondek, D. P. Siderovski, Nature 416, 878 (2002).
- 55. R. K. Sunahara, J. J. G. Tesmer, A. G. Gilman, S. R. Sprang, Science 278, 1943 (1997).
- We thank the laboratory of R. J. Lefkowitz (Duke University Medical Center) for Sf9 cell pellets bearing recombinant bovine GRK2 and for his insights regarding the potential role of GRK2 as a effector of  $G\alpha_{\rm cr}$ P. J. Hart for allowing us to perform preliminary characterization of the  $G\alpha_{i/q}\text{-}\mathsf{GRK2}\text{-}\mathsf{G}\beta\gamma$  crystals at the University of Texas Health Science Center at San Antonio x-ray facility, B. Kreutz (University of Illinois, Chicago) for help in generating the  $Ga_{i/a}$  construct, D. Lodowski and especially B. Earnest (UT Austin) for technical assistance, and R. Sterne-Marr and M. J. Ragusa (Siena College) for initial efforts to overexpress  $G\alpha_{\sigma}$ This work was supported by NIH grant HL071818, American Heart Association Scientist Development grant 0235273N and an American Cancer Society Research Scholar grant to J.J.G.T., and NIH grants GM61454 and NS41441 to T. Kozasa. T. Kawano gratefully acknowledges support from Y. Nakajima (NIH AG006093). The Advanced Light Source is supported by the Director, Office of Science, Office of Basic Energy Sciences, and Materials Sciences Division, of the U.S. Department of Energy under contract no. DE-AC03-76SF00098 at Lawrence Berkeley National Laboratory. Coordinates and diffraction data for the structure reported in this paper have been deposited in the Protein Data Bank as the entry 2BCJ.

## Supporting Online Material

www.sciencemag.org/cgi/content/full/310/5754/1686/ DC1

Materials and Methods

SOM Text Figs. S1 to S4

Table S1

Movies S1 and S2

15 August 2005: accepted 11 November 2005 10.1126/science.1118890